Orientation and Peptide−Lipid Interactions of Alamethicin Incorporated in Phospholipid Membranes: Polarized Infrared and Spin-Label EPR Spectroscopy

Derek Marsh*

Max-Planck-Institut für biophysikalische Chemie, Abt. Spektroskopie, 37070 Göttingen, Germany

Received July 8, 2008; Revised Manuscript Received November 20, 2008

ABSTRACT: Alamethicin is a 20-residue peptaibiotic that induces voltage-dependent ion channels in lipid membranes. The mode by which alamethicin inserts into membranes was investigated using measurements of peptide−lipid interactions by spin-label electron paramagnetic resonance (EPR) and of peptide orientation by polarized infrared (IR) spectroscopy. In fluid membranes, spin-labeled stearic acid shows no evidence of a specific motionally restricted population of lipid chains, such as that found at the intramembranous surface of integral membrane proteins or oligomeric assemblies of transmembrane α-helices. In agreement with recent results from TOAC-substituted alamethicin analogues, native alamethicin is predominantly monomeric in fluid lipid membranes and presents an intramembrane surface that integrates well with the lipid chains but is insufficiently extensive to induce specific motional restriction. Channel formation takes place by transient association of transmembrane monomers. In aligned fluid membranes, alamethicin exhibits a large tilt in short chain-length lipids that decreases first rapidly with increasing chain-length and then more gradually for the lipids with longer chains. This macroscopically low order contrasts with the high local order, relative to the local membrane normal, that is found by EPR for alamethicins spin-labeled with TOAC. The macroscopic behavior is consistent with predictions for the chain-length dependence of elastic bending fluctuations of the membrane surface, which was invoked recently to explain the spontaneous insertion of β-barrel proteins in short-chain lipid membranes.

Alamethicin is a peptaibol that induces voltage-dependent ion channel activity in lipid membranes (see, e.g., ref *1*). It consists of just 20 residues, including the C-terminal phenylalaninol (Fol),[1] which is scarcely sufficient to span the membrane, and it is almost entirely hydrophobic. The complete amino acid sequence of the predominant (ca. 75%) neutral species F50/5 is (*2*) Ac-Aib-Pro-Aib-Ala-Aib-Ala-Gln-Aib-Val-Aib-Gly-Leu-Aib-Pro-Val-Aib-Aib-Gln-Gln-Fol, where Aib is α-aminoisobutyric acid (2-MeAla). The peptide is, therefore, devoid of tryptophans or charged residues that could serve as interfacial membrane anchors. Nonetheless, consecutive steps in channel conductance support a model for the pores that consists of membrane-spanning oligomers (*3*), correlating with the transmembrane disposition of the spin-labeled monomers (*4, 5*). Recent EPR work on alamethicin spin-labeled substitutionally with the amino acid TOAC has revealed that it differs from other transmembrane peptides in its mode of membrane integration and that increases in the local tilt of the peptide molecular axis in response to decreasing membrane thickness are insufficient for maintaining hydrophobic matching (*6*).

It is, therefore, of considerable interest to investigate the way in which alamethicin is incorporated into phospholipid bilayer membranes by studying peptide−lipid interactions and additionally the orientation of the peptide in aligned membranes. In this work, I use polarized infrared spectroscopy to determine the conformation and alignment of alamethicin in membranes composed of disaturated phosphatidylcholines with different chain lengths. Further, I also study interactions of alamethicin with spin-labeled lipids in bilayer membranes by using EPR spectroscopy.

Measurements with macroscopically aligned samples are important because it was suggested recently that the local tilt of transmembrane polypeptides, which is determined partially by hydrophobic matching (*7*), is augmented by thermally excited elastic bending fluctuations of the entire membrane (*8*). These fluctuations both renormalize the elastic modulus for membrane area expansion (*9*), facilitating the insertion of transmembrane proteins, and give rise to a net inclination of the local membrane normal, or director, to which the molecular tilt of the peptide is referred (*8*).

A study of lipid−peptide interactions is significant because integral membrane proteins cause a motional restriction of the lipid chains in immediate contact with the transmembrane domain and this is detected by EPR as a specifically resolved population of spin-labeled lipids (*10*−*12*). On the other hand,

* To whom correspondence should be addressed. Telephone: +49 551 2011285. Fax: +49 551 2011501. E-mail: dmarsh@gwdg.de.

[1] Abbreviations: diC(10:0)PtdCho, 1,2-didecanoyl-*sn*-glycero-3-phosphocholine; diC(11:0)PtdCho, 1,2-diundecanoyl-*sn*-glycero-3-phosphocholine; diC(12:0)PtdCho, 1,2-dilauroyl-*sn*-glycero-3-phosphocholine; diC(13:0)PtdCho, 1,2-ditridecanoyl-*sn*-glycero-3-phosphocholine; diC(14:0)PtdCho, 1,2-dimyristoyl-*sn*-glycero-3-phosphocholine; diC(15:0)PtdCho, 1,2-dipentadecanoyl-*sn*-glycero-3-phosphocholine; diC(16:0)PtdCho, 1,2-dipalmitoyl-*sn*-glycero-3-phosphocholine; diC(17:0)PtdCho, 1,2-diheptadecanoyl-*sn*-glycero-3-phosphocholine; diC(18:1)PtdCho, 1,2-dioleoyl-*sn*-glycero-3-phosphocholine; 14-SASL, 14-(4,4-dimethyloxazolidinyl-*N*-oxyl)stearic acid; Hepes, *N*-(2-hydroxyethyl)piperazine-*N*′-2-ethanesulfonic acid; ATR, attenuated total reflectance; IR, infrared; EPR, electron paramagnetic resonance; Aib, α-aminoisobutyric acid; Fol, phenylalaninol; Phy, phytanoyl; TOAC, 2,2,6,6-tetramethylpiperidino-1-oxyl-4-amino-4-carboxylic acid.

10.1021/bi801279n CCC: $40.75
Published on Web 01/09/2009

a single transmembrane helix, such as the alamethicin monomer, has a cross-sectional area that is not much greater than that of a fluid diacyl lipid molecule (*13, 14*) and therefore may not give rise to the two-component signature in spin-label EPR that is characteristic of transmembrane proteins or peptide oligomers (see refs *15*−*17*). This work directly addresses these issues.

MATERIALS AND METHODS

Materials. Spin-labeled stearic acid (14-SASL) was synthesized according to the method of ref *18*. Symmetrical, disaturated phosphatidylcholines, diC(n_C:0)PtdCho, with odd and even chain lengths from 10 to 17 carbons, dioleoyl phosphatidylcholine [diC(18:1)PtdCho], and diphytanoylphosphatidylcholine (Phy_2PtdCho) were obtained from Avanti Polar Lipids (Alabaster, AL). Alamethicin from *Trichoderma viride* [a microheterogeneous mixture of neutral alamethicins F50 (see ref *2*)] and all other chemicals were from Sigma Chemical Co. (St. Louis, MO).

ATR Spectroscopy. Polarized ATR infrared spectra were recorded on a Bruker (Karlsruhe, Germany) IFS-25 Fourier transform spectrometer at a nominal resolution of 2 cm^{-1}. A horizontal ATR accessory from Specac (Orpington, U.K.) was used with a zinc selenide crystal (45° angle of incidence, six reflections). This was modified to seal the sample chamber hermetically from above and to thermostat the cell housing with internally circulating water from a temperature-controlled bath (Haake, Karlsruhe, Germany). The surface of the ATR crystal available for coating by the sample had dimensions of 8 mm × 45 mm. A germanium-mounted, wire-grid, linear polarizer (Specac) was used in the incident beam. Typically, 512 interferograms were co-added and Fourier-transformed after two levels of zero filling and apodization with a Blackman-Harris three-term function.

Samples containing 1 mg of lipid with alamethicin (predissolved in MeOH) at a peptide:lipid molar ratio of 1:50 were dried down on the ZnSe ATR crystal from solution in CH_2Cl_2. Spectra of the dry sample were then recorded with radiation polarized parallel and perpendicular to the plane of incidence. The sample was then hydrated with 70 μL of 150 mM NaCl in D_2O by incubation for 3−4 h above the chain-melting transition of the lipid bilayer, prior to recording the polarized ATR spectra at temperatures in the fluid and, subsequently, gel phases. After baseline subtraction, bands in the amide I (1590−1690 cm^{-1}) and CH stretching (2830−2975 cm^{-1}) regions were fitted with Lorentzian components by using nonlinear least-squares minimization. Dichroic ratios were calculated by using the integrated intensities of the α-helical bands in the 1655 cm^{-1} region and those of the CH antisymmetric stretching bands in the region of 2920 cm^{-1}. To calculate molecular orientations from dichroic ratios, strengths of the infrared electric field components were obtained from the thick film approximation, appropriate to the amount of material used: $E_x^2/E_y^2 = 0.450$ and $E_z^2/E_y^2 = 1.550$ for a 45°-cut zinc selenide ATR crystal. The thickness of the hydrated sample was ∼10 μm, and the penetration depth of the evanescent radiation is ∼0.9 μm at 1650 cm^{-1}.

EPR Spectroscopy. EPR spectra were recorded on Varian (Palo Alto, CA) Century Line and Bruker (Rheinstetten, Germany) EMX 9-GHz spectrometers with rectangular cavities and nitrogen gas-flow temperature regulation. Samples were accommodated in 1-mm diameter glass capillaries, which were placed in a standard quartz EPR tube that contained light silicone oil for thermal stability. A solution of alamethicin (predissolved in MeOH) with 1.2 mg of diC(14:0)PtdCho and 1 mol % 14-SASL at the desired peptide:lipid ratio in CH_2Cl_2 was dried down under nitrogen and then incubated under vacuum overnight. The dry sample was hydrated with excess buffer [40 μL of 20 mM Hepes (pH 7.8)] by vortex mixing above the chain-melting temperature of diC(14:0)PtdCho. This was then pelleted in the glass capillary by using a benchtop centrifuge. Excess supernatant was removed, and the capillary was flame-sealed.

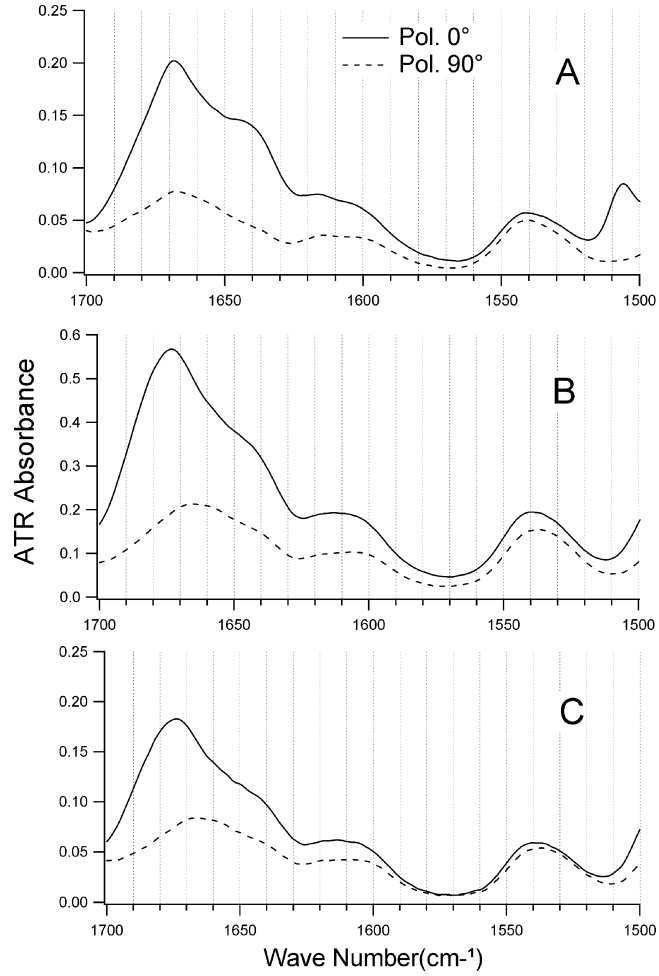

FIGURE 1: Polarized ATR-FTIR spectra (amide I and amide II regions) of alamethicin (1:50 molar ratio) in aligned membranes of (A) diC(10:0)PtdCho, (B) diC(15:0)PtdCho, and (C) diC(17:0)PtdCho at 10 °C. Solid lines correspond to parallel polarization and dashed lines to perpendicular polarization of the incident radiation.

RESULTS

Polarized IR Spectra of Alamethicin in PtdCho. Figure 1 shows the amide I and amide II regions from the polarized ATR spectra of alamethicin in aligned diC(10:0)PtdCho, diC(15:0)PtdCho, and diC(17:0)PtdCho membranes dispersed in D_2O. The intensity is low in the amide II region because D−H exchange shifts the predominantly N−H stretch mode to much lower frequencies. The amide I band (predominantly C═O stretch) is shifted only little and displays a pronounced dichroism that differs between the lipid hosts.

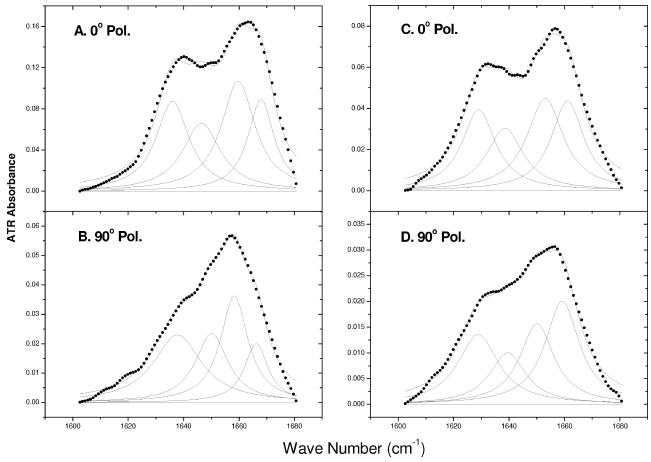

FIGURE 2: Amide I region from polarized ATR-FTIR spectra of alamethicin (1:50 molar ratio) in aligned membranes of diC(15:0)PtdCho lipid (●). Spectra A and B were recorded in the gel phase at 10 °C, whereas spectra C and D were recorded in the fluid phase at 43 °C. The spectra in the top panels (A and C) correspond to parallel polarization and those in the lower panels (B and D) to perpendicular polarization of the incident radiation. Note the different ordinate scales. The solid lines correspond to the least-squares fit, with the bands obtained from the band fitting analysis shown below the experimental spectrum.

Figure 2 shows band fitting of the amide I region in the polarized ATR spectra of alamethicin in hydrated aligned membranes of dipentadecanoylphosphatidylcholine [diC(15:0)PtdCho]. Spectra are shown from membranes in the gel state (Figure 2A,B) and in the fluid state (Figure 2C,D), below and above the chain-melting transition at 35 °C. The amide I spectra consist of a major peak at 1655−1660 cm^{-1}, at the upper end of the range expected for α-helices in D_2O (cf. refs *19* and *20*), and a pronounced shoulder at a lower frequency in the region of 1635−1640 cm^{-1}.

Band fitting determines the intensities of the components contributing to the amide I band shape for each polarization (see Figure 2). To obtain the true absorbed intensity, it is necessary to combine absorbances, $A_{||}$ and $A_{\perp}$, for parallel and perpendicular polarized radiation, respectively (*21*). The appropriate admixture of $A_{\perp}$ with $A_{||}$ that allows quantitatively for the spectral dichroism is $A_{||} + (2E_z^2/E_y^2 - E_x^2/E_y^2)A_{\perp}$, in the geometry used here. The fractional population of a particular component j is therefore given by

$$f_j = \frac{A_{||,j} + \left(2\frac{E_z^2}{E_y^2} - \frac{E_x^2}{E_y^2}\right)A_{\perp,j}}{\sum_j \left[A_{||,j} + \left(2\frac{E_z^2}{E_y^2} - \frac{E_x^2}{E_y^2}\right)A_{\perp,j}\right]} \quad (1)$$

where $A_{||,j}$ and $A_{\perp,j}$ are the integrated absorbances of component j that are obtained from band fitting to the parallel and perpendicularly polarized spectra, respectively. Table 1 gives the corresponding results of band fitting for the amide I region from alamethicin in disaturated phosphatidylcholines of different chain lengths. Fitting data are given for hydrated membranes in both the gel and fluid phases, recorded at temperatures of 10 and 36 °C or higher, respectively. The relative conformational populations are seen to be similar in the fluid and gel phases of a given lipid. Note that the band fitting reveals components in the normal range for α-helices around 1650 cm^{-1}, in addition to those at higher frequencies. The distribution probably reflects imperfections in the α-helix.

Table 1: Band Fitting of the Polarized ATR Spectra from the Amide I Band of Alamethicin in Hydrated Disaturated Phosphatidylcholines, diC(n_C:0)PtdCho, with Different Chain Lengths, n_C, in the Gel and Fluid Phases

	gel		fluid	
	position (cm^{-1})	normalized area (%)[a]	position (cm^{-1})	normalized area (%)[a]
C(10:0)			1628	18
			1637	23
			1647	21
			1656	24
			1663	14
C(11:0)			1630	32
			1643	25
			1654	28
			1662	15
C(12:0)			1630	27
			1642	28
			1654	25
			1662	21
C(13:0)	1628	18	1630	21
	1639	24	1643	29
	1653	38	1655	35
	1663	20	1665	15
C(14:0)	1630	29	1631	29
	1643	27	1642	22
	1655	33	1654	33
	1665	11	1664	16
C(15:0)	1628	28	1631	33
	1638	20	1645	25
	1651	21	1656	27
	1659	30	1664	15
C(16:0)	1630	26	1630	29
	1648	18	1649	19
	1659	27	1659	25
	1663	28	1663	27
C(17:0)	1637	21	1635	20
	1650	25	1646	24
	1660	35	1658	37
	1669	19	1666	19

[a] Relative band intensities are obtained by combining integrated absorbances, $A_{||}$ and $A_{\perp}$, with radiation polarized parallel and perpendicular, respectively, to the plane of the incident beam, according to eq 1.

Amide Dichroism of Alamethicin in PtdCho. Figure 3 shows the temperature dependences of the dichroic ratio, R_I, and frequency of the band maximum, ν_I, of the amide I band from alamethicin at ca. 1660 cm^{-1} in diC(15:0)PtdCho membranes hydrated in D_2O. For comparison, corresponding values, R_{CH} and ν_{CH}, for the CH_2 antisymmetric stretch band of the lipid chains are also included in the figure. All values exhibit a discontinuity in the region of the lipid chain-melting transition, which occurs at ca. 34−35 °C in bilayers of diC(15:0)PtdCho that do not contain peptide (*14*). Interestingly, the changes in the peptide precede those of the bulk lipid chains, indicating that alamethicin exhibits a preference for the fluid phase over the gel phase in diC(15:0)PtdCho. This suggests that the length of the alamethicin molecule, which is mostly apolar, is comparable to the hydrophobic thickness of fluid diC(15:0)PtdCho bilayers, consistent with recent conclusions about the location of TOAC-substituted alamethicins in phosphatidylcholines of different chain lengths (*6*).

Figure 4 gives the dichroic ratios of the α-helical components at ca. 1655/1660 cm^{-1} in the amide I band from alamethicin in hydrated membranes, as a function of chain length, n_C, of the

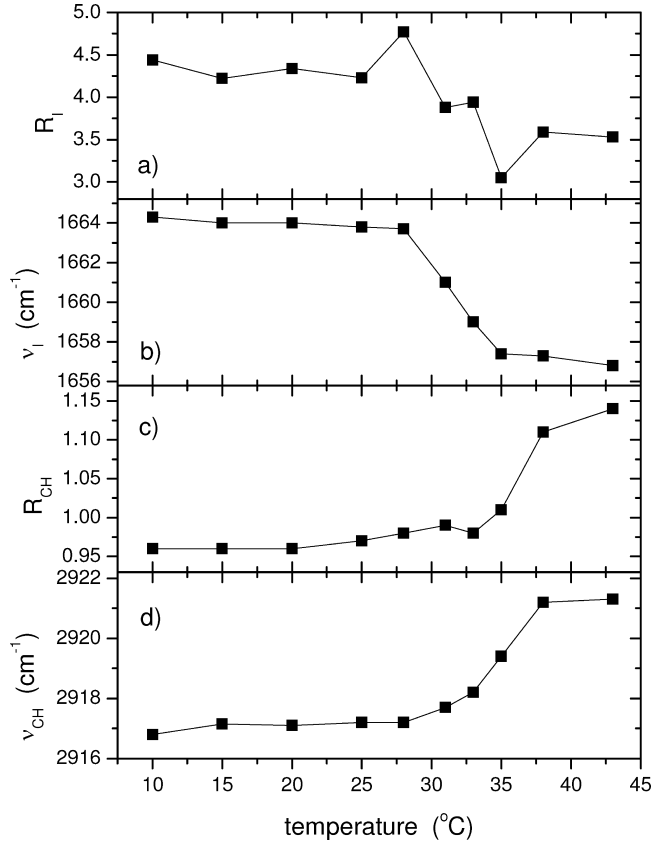

FIGURE 3: Temperature dependences of (a and c) dichroic ratios, R, and (b and d) band maxima, ν, from (a and b) the amide I band of alamethicin at ca. 1660 cm^{-1} and (c and d) the lipid chain CH_2 antisymmetric stretch band at ca. 2920 cm^{-1} in 1:50 mol/mol alamethicin/diC(15:0)PtdCho membranes. Membranes are hydrated in 150 mM NaCl/D_2O (pD 6.0).

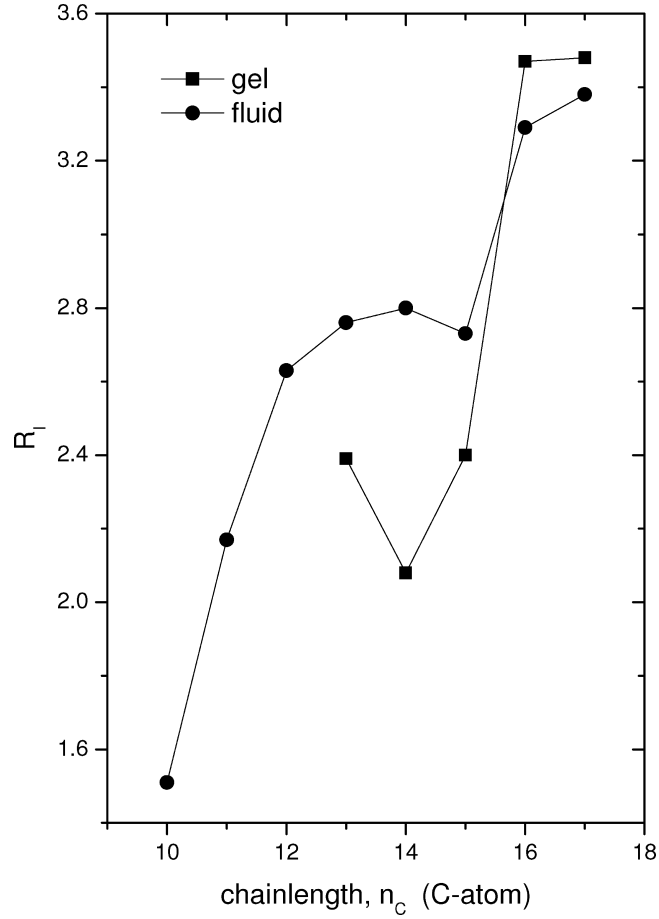

FIGURE 4: Dependence of the dichroic ratios from the amide I band of alamethicin at ca. 1655/1660 cm^{-1} on lipid chain length, n_C, of the diC(n_C:0)PtdCho membrane in which the peptide is incorporated. Dichroic ratios are given for the samples in the gel phase [10 °C (■)] and in the fluid phase [36 °C, or 43, 46, and 58 °C for C(15:0), C(16:0), and C(17:0), respectively (●)]. Membranes are hydrated in 150 mM NaCl/D_2O (pD 6.0).

disaturated PtdCho lipid. Values are given for membranes at a fixed temperature in the gel phase (10 °C; cf. Figure 3a) and at a higher temperature corresponding to the fluid phase above the lipid chain-melting transition (at 36 °C for n_C values of 10−14 and at 43, 46, and 58 °C for n_C values of 15, 16, and 17, respectively). The general trend is an increase in the amide I dichroic ratio with an increase in lipid chain length, with an additional step around the position of hydrophobic matching when $n_C \approx 15.5$ (cf. ref *6*).

The order parameter of the molecular axis of alamethicin is related to the measured dichroic ratio, $R(\Theta)$, according to (*22*)

$$\langle P_2(\cos\gamma)\rangle = \frac{E_x^2/E_y^2 + E_z^2/E_y^2 - R(\Theta)}{P_2(\cos\Theta)[E_x^2/E_y^2 - 2E_z^2/E_y^2 - R(\Theta)]} \quad (2)$$

where γ is the orientation of the molecular axis relative to the normal to the orienting substrate (i.e., the ATR plate) and Θ is the orientation of the transition moment relative to the molecular axis (see Figure 5). For the amide I band of an α-helix, which is a superposition of the $\nu_{||}(0,\pi)$ and $\nu_{\perp}(\pi,0)$ modes (*22, 23*), the orientation of the net transition moment is $\Theta = 38°$ (*24, 25*). Order parameters are related to the molecular tilt angle by

$$\langle P_2(\cos\gamma)\rangle = \frac{1}{2}(3\langle\cos^2\gamma\rangle - 1) \quad (3)$$

where angular brackets indicate summation over the (normalized) orientational distribution in γ. These order parameters are a composite of the molecular orientation in the membrane and the degree of alignment of the membrane relative to the surface of the ATR crystal, which can be parametrized by a multiplicative factor, f (see below). Effective tilt angles, γ_{eff}, are obtained from $\langle\cos^2\gamma\rangle$ by assuming a singular value of γ. Table 2 lists values of the order parameter, $\langle P_2(\cos\gamma)\rangle$, deduced from eq 2, and the effective tilt that is obtained from eq 3, for alamethicin in fluid- and gel-state phosphatidylcholine membranes of different chain lengths. The trend is similar to that of the dichroic ratios: the order parameters increase and the tilt angles decrease with an increase in lipid chain length. Interestingly, the degree of order in the longer-chain *cis*-monounsaturated diC(18:1)PtdCho is similar to that of diC(17:0)PtdCho, whereas that in the saturated but extensively methyl-branched Phy_2PtdCho is similar to that in the much shorter straight-chain diC(11:0)PtdCho.

Lipid Chain Dichroism in Alamethicin/PtdCho Membranes. Order parameters, $\langle P_2(\cos\gamma_{ch})\rangle$, and effective tilt angles, γ_{ch}, of the lipid chains, relative to the substrate normal, are given in Table 3. These values are derived from the dichroic ratios of the CH_2 antisymmetric stretch bands at ca. 2920 cm^{-1} (see Figure 3c). The transition moment for CH_2 stretch vibrations is perpendicular to the chain axis, and the order parameter of the latter is given by eq 2 with a Θ of 90°. The order parameters in the fluid phase are smaller

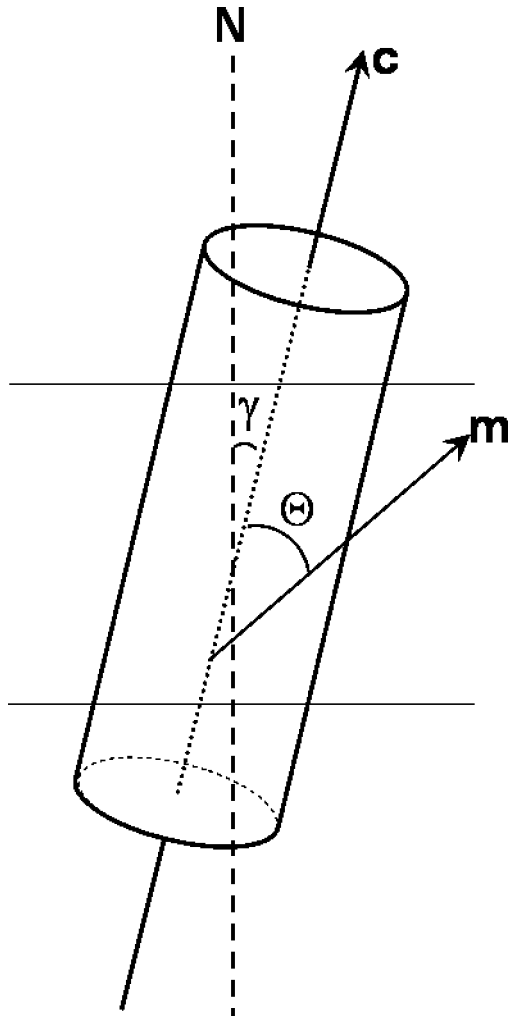

FIGURE 5: Orientation of the amide I [superposition of the $\nu_{||}(0,\pi)$ and $\nu_{\perp}(\pi,0)$ modes] transition moment, **m**, of alamethicin in a lipid membrane. The helix long axis, **c**, is tilted at an angle γ to the membrane normal, **N**. The amide transition moment is oriented at a fixed angle, Θ, to the helix axis.

Table 2: Order Parameters, $\langle P_2(\cos\gamma)\rangle$, and Mean Effective Inclination, γ_{eff}, of Alamethicin in Membranes of Diacyl Phosphatidylcholines, diC(n_C:*x*)PtdCho, with Different Chain Lengths, n_C, in the Gel and Fluid Phases

	gel[a]		fluid[a]	
	$\langle P_2(\cos\gamma)\rangle$	γ_{eff} (deg)	$\langle P_2(\cos\gamma)\rangle$	γ_{eff} (deg)
C(10:0)			−0.27	67
C(11:0)			0.08	51
C(12:0)			0.28	44
C(13:0)	0.18	48	0.33	42
C(14:0)	0.04	53	0.34	42
C(15:0)	0.18	48	0.31	43
C(16:0)	0.56	33	0.50	35
C(17:0)	0.56	33	0.53	34
C(18:1)			0.57	33
Phy[b]			0.01	54

[a] Gel phase at 10 °C; fluid phase at 36 °C [C(10:0)−C(14:0)], 43 °C [C(15:0)], 46 °C [C(16:0)], 58 °C [C(17:0)], or 20 °C [C(18:1) and Phy]. [b] Phy, phytanoyl chains.

than those in the gel phase, corresponding to chain fluidization; γ_{ch} is then an effective value that represents the mean order parameter of the individual chain segments that are undergoing rapid rotational isomerism in the fluid phase. In the gel phase, the values of γ_{ch} correspond to the static tilt of the long axis of the nearly all-*trans* chains. For comparison, the tilt of the chains of disaturated phosphatidylcholines in gel-phase bilayers that is determined from X-ray diffraction lies in the range of 30−35° (*14*). The values of γ_{ch} that are derived for the gel-phase membranes in Table 3 are close to this range and therefore indicate that the lipid membranes containing alamethicin are reasonably well aligned.

Table 3: Order Parameters, $\langle P_2(\cos\gamma_{ch})\rangle$, and Effective Tilts, γ_{ch}, of Lipid Chains in Aligned Membranes of Disaturated Phosphatidylcholines, diC(n_C:0)PtdCho, Containing Alamethicin (1:50 molar ratio), in the Gel and Fluid Phases[a]

	gel[b]		fluid[b]	
	$\langle P_2(\cos\gamma_{ch})\rangle$	γ_{ch} (deg)	$\langle P_2(\cos\gamma_{ch})\rangle$	γ_{ch} (deg)
C(10:0)			0.41	39
C(11:0)			0.53	34
C(12:0)			0.42	39
C(13:0)	0.49	36	0.38	40
C(14:0)	0.49	36	0.30	43
C(15:0)	0.56	33	0.42	38
C(16:0)	0.41	38	0.49	36
C(17:0)	0.65	29	0.53	34

[a] Deduced from the dichroism of the CH_2 antisymmetric stretch band at 2920 cm^{-1}. [b] Gel phase at 10 °C; fluid phase at 36 °C [C(10:0)−C(14:0)], 43 °C [C(15:0)], 46 °C [C(16:0)], or 58 °C [C(17:0)].

EPR of Spin-Labeled Lipid. Figure 6 shows the EPR spectra of the stearic acid spin-label 14-SASL in diC(14:0)PtdCho/alamethicin membranes at peptide:lipid molar ratios of 1:25, 1:12, and 1:6, as indicated. Spectra are given for sample temperatures in the range of 10−35 °C, which encompasses both the gel and fluid phases of the lipid membrane. The spectral line shapes depend upon the peptide:lipid ratio in the pretransitional region (15−20 °C) but are rather similar for the different samples at a given temperature in the fluid phase. Only a small increase in line widths with an increase in alamethicin:lipid ratio is observed in the latter case. In particular, the spectra in the fluid phase show no indication of an additional, peptide-dependent motionally restricted component, as observed with integral membrane proteins (e.g., refs *26*−*28*).

In the intermediate gel phase, the EPR spectra are characterized by two components from lipids of differing mobility, which are indicated by arrows in the low field of the spectra at 15 and 20 °C. The situation is complex, because coexisting spectral components are found even in the absence of peptide, in the gel phase. The inset of Figure 6 gives the dependence of the ratio of line heights for the immobile and mobile components in the low-field region on the peptide:lipid ratio. The response is biphasic. Initially, the population of motionally restricted lipid increases with an increase in peptide content, which might be expected if the peptide forms oligomers that present an immobilizing surface to the lipid chains. At higher concentrations, however, the peptide assemblies cause a reduction in the population of immobilized lipids, presumably from the effect of higher peptide concentrations on the bulk phase properties of the gel-phase lipid.

Figure 7 shows chain melting (i.e., gel−fluid) phase transition curves for diC(14:0)PtdCho bilayers with increasing alamethicin content. These confirm that alamethicin/diC(14:0)PtdCho membranes still undergo cooperative chain melting at peptide:lipid molar ratios of up to 1:6. The EPR line height is normalized to the double integral of the first-derivative spectrum. Increases in normalized intensity with

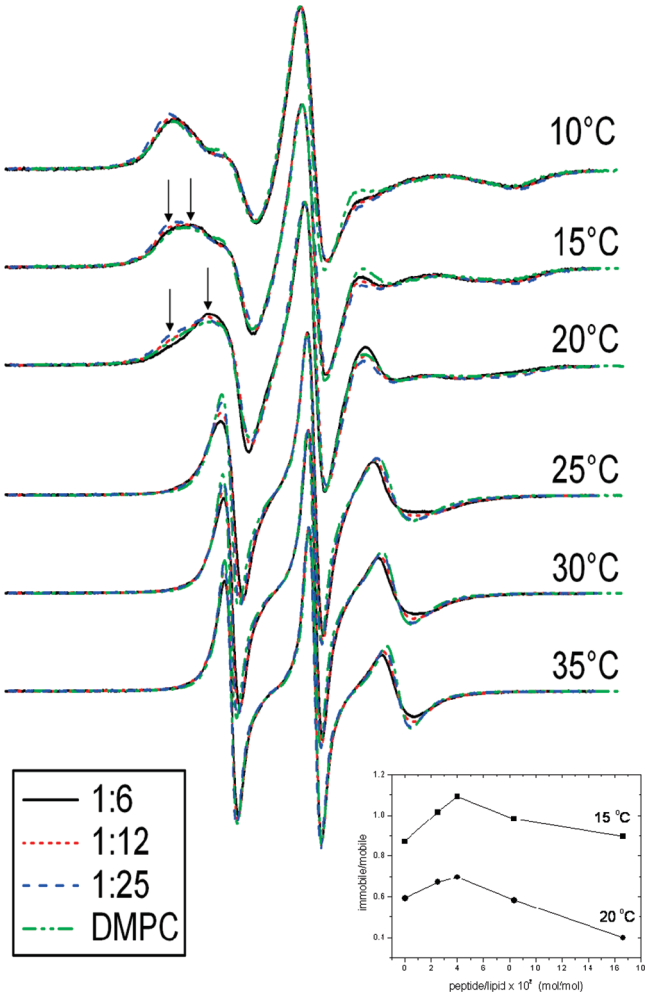

FIGURE 6: EPR spectra of spin-labeled stearic acid, 14-SASL, in bilayer membranes of diC(14:0)PtdCho containing alamethicin at peptide:lipid molar ratios of 1:25 (---), 1:12 (•••), and 1:6 (—), at the temperatures indicated. Spectra in diC(14:0)PtdCho lipid alone are given by dashed-and-dotted lines. The total scan width was 100 G. The inset shows the dependence on peptide:lipid ratio of the line heights of the immobile and mobile components of the low-field ($m_I = +1$) hyperfine manifold (indicated by arrows) at 15 and 20 °C.

an increase in temperature therefore reflect the progressive line narrowing that takes place as a result of chain dynamics in the fluid phase.

DISCUSSION

Conformation of Alamethicin. The amide I region in the IR spectrum from alamethicin, including that of the peptide in methanol, is characterized by a major band in the conventional range for α-helices at 1655−1660 cm^{-1} [overlapping $\nu_{\parallel}(0,\pi)$ and $\nu_{\perp}(\pi,0)$ modes (*23*)], together with shoulders in the low-frequency region at ≤1640 cm^{-1} (*29*−*31*). The latter do not resemble the sharp bands in the 1620−1630 cm^{-1} region that are characteristic of β-barrel or β-sheet membrane proteins (*20, 32*−*35*), particularly in the dry state (data not shown). On the other hand, low-frequency amide I bands in the region of 1630−1640 cm^{-1} have been attributed either to 3_{10}-helices (*36, 37*) or to solvent-exposed α-helices that participate in bifurcated H-bonds (*37, 38*). The crystal structure of alamethicin F30 that is obtained from X-ray diffraction is predominantly helical, with an N-terminal

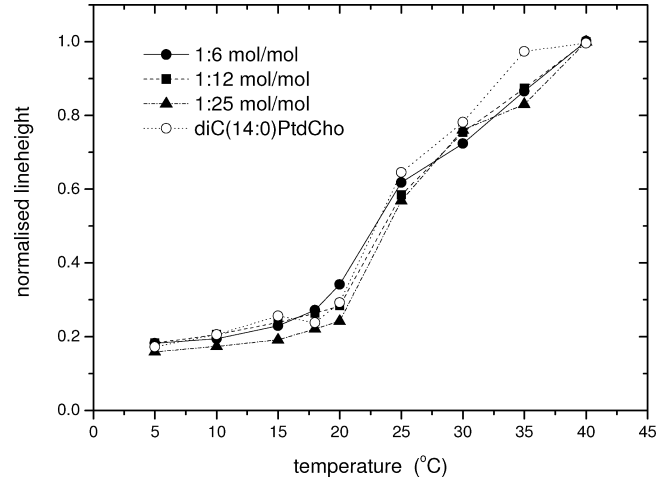

FIGURE 7: Temperature dependence of the central line height in the EPR spectrum of the 14-SASL spin-label in diC(14:0)PtdCho membranes containing alamethicin at peptide:lipid molar ratios of 1:6 (●), 1:12 (■), and 1:25 (▲), as indicated. Data for the diC(14:0)PtdCho lipid alone are also given (○). Line heights are scaled to the double-integrated intensity of the normal, first-derivative EPR spectrum.

α-helix and a C-terminal domain beyond Pro^{14} that contains 3_{10}-helical elements (*39*). Also, a mixed α/3_{10}-helical structure is found in one of the crystal conformers of an alamethicin F50/5 analogue (*40*). Note that the CO stretch vibrations of Gln side chains absorb in the 1635−1654 cm^{-1} region when completely hydrogen bonded in D_2O but could lie 50 cm^{-1} higher for a non-H-bonded state in the membrane interior (*41*). In D_2O, the molar absorbance of a Gln side chain is similar to that of the peptide amide I mode (*42*). Therefore, at low frequencies, Gln side chains could contribute a fraction of 3/23 (13%) to the total intensity in the entire amide I region. Correspondingly, the relative intensity of the bands around 1665 cm^{-1} in Table 1 would be corrected up by a factor of 23/20 (1.15).

Because alamethicin is mostly buried in the membrane (*5, 6*), it is reasonable to assign the low-frequency bands in Table 1 partly to 3_{10}-helix, partly to side chains, and the remainder (as well as the high-frequency bands) to α-helix. Such an assignment is consistent with the finding that the intensity of the low-frequency amide I bands is reduced for an alamethicin analogue with the Aib residues replaced with Leu, which is expected to promote formation of α-helices at the expense of 3_{10}-helix (*30*). Note that the C^{α}-tetrasubstituted Aib residue favors formation of 3_{10}-helices (*43, 44*). On this basis, the absolute maximum content of 3_{10}-helix that alamethicin can have in the different phosphatidylcholine host lipids ranges progressively from 56% in diC(10:0) to 36% in diC(17:0) phosphatidylcholine, with a mean value of 46 ± 7%, after the contribution from Gln side chains has been subtracted. Correspondingly, the minimum content of α-helix ranges from 44% in diC(10:0) to 64% in diC(17:0) phosphatidylcholine, with a mean value of 54 ± 7%. For reference, alamethicin F30 crystallized from methanol contains only one or two residues of 3_{10}-helix, i.e., ca. 10% of the total helix (*39*), and solid-state NMR studies in lipid membranes are consistent with a largely linear α-helical structure (*45*). For the reasons given above, the values for 3_{10}-helical content estimated from the 1630−1640 cm^{-1} IR bands are an absolute upper limit and likely to be a considerable overestimate. The increasing intensity of these

bands with a decrease in membrane thickness (see Table 1) is consistent with a substantial contribution from solvent-exposed α-helices that could absorb in the 1630−1640 cm^{-1} range. From the comparisons with X-ray and NMR structures, it seems clear that the 1630−1640 cm^{-1} bands in alamethicin should be attributed primarily to α-helices participating in bifurcated hydrogen bonds, rather than to 3_{10}-helices.

Alamethicin Orientation. The effective order parameters of the alamethicin backbone relative to the local membrane director have been measured by EPR with TOAC-substituted alamethicins (*6*). These evidence a high degree of local order, even at high temperatures in the fluid phase, with local effective tilts ($\gamma_{eff,loc}$) varying from 23° for diC(10:0)PtdCho to 13° for diC(17:0)PtdCho at 75 °C. Similarly, only small local tilts that are incompletely responsive to hydrophobic mismatch are found for synthetic Leu-Ala WALP and KALP α-helical peptides (*16, 17, 46*). In contrast, the total effective tilts measured here for alamethicin by polarized IR in aligned samples are much larger: $\gamma_{eff} = 54°$ and 40° for diC(10:0)PtdCho and diC(17:0)PtdCho, respectively, in the fluid phase (see Table 2).

In aligned membranes, the increasing orientational order, or decreasing tilt, of β-barrel proteins with an increase in the chain length of the host lipid (also measured by polarized IR) has been interpreted in terms of elastic bending fluctuations of the membrane, which modulate the orientation of the protein relative to the aligning ATR substrate (*8*). This treatment predicts that the local membrane director fluctuates according to (*8*)

$$1 - \langle P_2(\cos \gamma_o)\rangle \propto 1/k_c \quad (4)$$

where k_c is the bending rigidity or mean elastic curvature modulus of the membrane (*47*). The curvature modulus scales with the thickness, d_c, of the hydrophobic core of the membrane according to

$$k_c \approx \frac{1}{4} K_A d_c^2 \propto (n_C - 1)^2 \quad (5)$$

where K_A is the area expansion modulus of the membrane. Figure 8 shows the dependence of the alamethicin order parameters on lipid chain length. These data have been corrected for the local order, $\langle P_2(\cos \gamma_{loc})\rangle$, according to the addition theorem for spherical harmonics with axial symmetry:

$$\langle P_2(\cos \gamma_o)\rangle = \langle P_2(\cos \gamma)\rangle / \langle P_2(\cos \gamma_{loc})\rangle \quad (6)$$

to yield the intrinsic contribution, $\langle P_2(\cos \gamma_o)\rangle$, from elastic director fluctuations. The solid line in Figure 8 represents a nonlinear, least-squares fit to the measured order parameters with the dependence on n_C that is predicted from eqs 4 and 5 for elastic bending fluctuations of the lipid membrane. This is capable of describing the chain-length dependence reasonably well, without additional static or dynamic disorder, i.e., with $f \sim 1.0$ (see Figure 8).

Thus, the results from membranes aligned on the ATR substrate, relative to the (local) molecular order parameter measurements on TOAC-substituted alamethicin analogues that were reported previously (*6*), support the general model for peptide tilting based on thermally driven elastic bending fluctuations. This mechanism was proposed originally to account for the very steep chain length dependence of

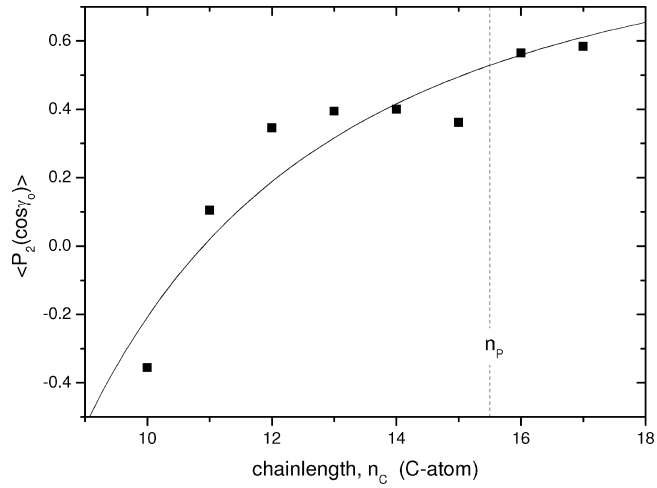

FIGURE 8: Dependence of the order parameters, $\langle P_2(\cos \gamma_o)\rangle$, for director fluctuations on lipid chain length, n_C, of the fluid-phase diC(n_C:0)PtdCho membrane in which alamethicin is incorporated. The experimental order parameters for alamethicin, $\langle P_2(\cos \gamma)\rangle$, from Table 2 are corrected by using EPR measurements of the local order, $\langle P_2(\cos \gamma_{loc})\rangle$, of alamethicin in the membrane (*6*) to yield the intrinsic contribution from director fluctuations according to eq 6. The vertical dashed line corresponds approximately to the lipid chain length, n_P, expected to give hydrophobic matching with alamethicin (*6*). The solid line is a nonlinear least-squares fit of the chain length dependence $P_2 \sim [1 - B/(n_C - 1)^2] \times f$ that is predicted from eqs 4 and 5 for elastic bending fluctuations of the membrane. The optimized value of f, 0.99 ± 0.11, allows for the possibility that the sample may not be perfectly aligned.

spontaneous folding and insertion of β-barrel proteins in lipid membranes (*8*) and is consistent with dichroism measurements on such outer membrane proteins (*33, 34, 48*). Note that a similar principle should apply to all angle-dependent measurements on aligned fluid membranes at full hydration. Recent IR dichroism measurements on transmembrane peptides from the vacuolar ATPase, for example, reveal effective tilts that are greater than those required for complete hydrophobic matching, which is fully in line with the interpretation presented here (*20*).

Lipid−Peptide Interactions. The lack of a motionally restricted component, in addition to that of the fluid bilayer lipids, in the EPR spectra of 14-SASL, even at the highest peptide:lipid ratios, indicates that alamethicin is integrated in fluid-phase diC(14:0)PtdCho membranes as a monomer. Oligomers of single-spanning helices are found to give rise to a motionally restricted population of spin-labeled lipids, much as do multiple-spanning integral proteins (*20, 49, 50*). Single bitopic helices, however, appear mostly to present an insufficiently extensive intramembranous surface to produce a specifically resolved motionally restricted population of spin-labeled lipid chains (*15−17*). A notable exception is, nonetheless, the L37A mutant of phospholamban in which disruption of the leucine zipper produces a monomeric species and motionally restricted lipids are observed (*51*). This is probably related to the particular primary structure of phospholamban, and in general, motionally restricted lipids are not necessarily expected to be resolved with single transmembrane helices, rather like the situation that exists with the rigid steroid cholesterol (*52, 53*).

The conclusion that native alamethicin is present predominantly as a monomer in fluid lipid membranes is consistent with the lack of spin−spin interactions between spin-labeled alamethicin analogues (*4*) and their submicrosecond rota-

tional correlation times (*5*), at least in the absence of a membrane potential. Alamethicin therefore does not form highly stable oligomeric assemblies in fluid lipid membranes. At membrane concentrations often used in electrophysiological experiments, the ion-conducting pores are transient species (*54*). This opening of voltage-dependent ion channels does not, however, occur via conformational transitions or rearrangements within stable channel assemblies. Note that, in contrast, the transmembrane current density mediated by alamethicin increases dramatically when it enters the lipid gel phase (*55*), where strong spin−spin interactions are observed between alamethicin analogues that contain the TOAC spin-label (*5*). Stable oligomer formation in the gel phase is suggested also here from the initial increase in the population of motionally restricted lipids by alamethicin. Thus, in normal fluid membranes, the bulk of alamethicin is monomeric, and pore formation and growth occur via transient association of peptide monomers, in accordance with the dependence on lipid structure (see, e.g., refs *56* and *57*), not from conformational transitions within preexisting alamethicin aggregates.

ACKNOWLEDGMENT

I thank Frau B. Freyberg for skilled technical assistance and Frau B. Angerstein for spin-label synthesis.

REFERENCES

1. Marsh, D. (1996) Peptide models for membrane channels. *Biochem. J. 315*, 345–361.
2. Kirschbaum, J., Krause, C., Winzheimer, R., and Brückner, H. (2003) Sequences of alamethicins F30 and F50 reconsidered and reconciled. *J. Pept. Sci. 9*, 799–809.
3. Boheim, G., and Kolb, H.-A. (1978) Analysis of the multi-pore system of alamethicin in a lipid membrane. I. Voltage-jump current-relaxation measurements. *J. Membr. Biol. 38*, 99–150.
4. Barranger-Mathys, M., and Cafiso, D. S. (1996) Membrane structure of voltage-gated channel forming peptides by site-directed spin-labeling. *Biochemistry 35*, 498–505.
5. Marsh, D., Jost, M., Peggion, C., and Toniolo, C. (2007) TOAC spin labels in the backbone of alamethicin: EPR studies in lipid membranes. *Biophys. J. 92*, 473–481.
6. Marsh, D., Jost, M., Peggion, C., and Toniolo, C. (2007) Lipid chainlength dependence for incorporation of alamethicin in membranes: EPR studies on TOAC-spin labelled analogues. *Biophys. J. 92*, 4002–4011.
7. Marsh, D. (2008) Energetics of hydrophobic matching in lipid-protein interactions. *Biophys. J. 94*, 3996–4013.
8. Marsh, D., Shanmugavadivu, B., and Kleinschmidt, J. H. (2006) Membrane elastic fluctuations and the insertion and tilt of β-barrel proteins. *Biophys. J. 91*, 227–232.
9. Marsh, D. (1997) Renormalization of the tension and area expansion modulus in fluid membranes. *Biophys. J. 73*, 865–869.
10. Marsh, D., and Horváth, L. I. (1998) Structure, dynamics and composition of the lipid-protein interface. Perspectives from spin-labelling. *Biochim. Biophys. Acta 1376*, 267–296.
11. Marsh, D., and Páli, T. (2004) The protein-lipid interface: Perspectives from magnetic resonance and crystal structures. *Biochim. Biophys. Acta 1666*, 118–141.
12. Esmann, M., and Marsh, D. (2006) Lipid-protein interactions with the Na,K-ATPase. *Chem. Phys. Lipids 141*, 94–104.
13. Marsh, D. (1997) Stoichiometry of lipid-protein interaction and integral membrane protein structure. *Eur. Biophys. J. 26*, 203–208.
14. Marsh, D. (1990) *Handbook of Lipid Bilayers*, CRC Press, Boca Raton, FL.
15. Pérez-Gil, J., Casals, C., and Marsh, D. (1995) Interactions of hydrophobic lung surfactant proteins SP-B and SP-C with dipalmitoylphosphatidylcholine and dipalmitoylphosphatidylglycerol bilayers studied by electron spin resonance spectroscopy. *Biochemistry 34*, 3964–3971.
16. de Planque, M. R. R., Greathouse, D. V., Koeppe, R. E., II, Schäfer, H., Marsh, D., and Killian, J. A. (1998) Influence of lipid/peptide hydrophobic mismatch on the thickness of diacylphosphatidylcholine bilayers. A ^{2}H NMR and ESR study using designed transmembrane α-helical peptides and gramicidin A. *Biochemistry 37*, 9333–9345.
17. de Planque, M. R. R., Kruijtzer, J. A. W., Liskamp, R. M. J., Marsh, D., Greathouse, D. V., Koeppe, R. E., II, De Kruijff, B., and Killian, J. A. (1999) Different membrane anchoring positions of tryptophan and lysine in synthetic transmembrane α-helical peptides. *J. Biol. Chem. 274*, 20839–20846.
18. Marsh, D., and Watts, A. (1982) Spin-labeling and lipid-protein interactions in membranes. In *Lipid-Protein Interactions* (Jost, P. C., and Griffith, O. H., Eds.) Vol. 2, pp 53−126, Wiley-Interscience, New York.
19. Holzenburg, A., Jones, P. C., Franklin, T., Páli, T., Heimburg, T., Marsh, D., Findlay, J. B. C., and Finbow, M. E. (1993) Evidence for a common structure for a class of membrane channels. *Eur. J. Biochem. 213*, 21–30.
20. Kóta, Z., Páli, T., Dixon, N., Kee, T. P., Harrison, M., Findlay, J. B. C., Finbow, M. E., and Marsh, D. (2008) Incorporation of transmembrane peptides from the vacuolar H^+-ATPase in phospholipid membranes: Spin-label electron paramagnetic resonance and polarized infrared spectroscopy. *Biochemistry 47*, 3937–3949.
21. Marsh, D. (1999) Quantitation of secondary structure in ATR infrared spectroscopy. *Biophys. J. 77*, 2630–2637.
22. Marsh, D. (1997) Dichroic ratios in polarized Fourier transform infrared for nonaxial symmetry of β-sheet structures. *Biophys. J. 72*, 2710–2718.
23. Miyazawa, T. (1960) Perturbation treatment of the characteristic vibrations of polypeptide chains in various configurations. *J. Chem. Phys. 32*, 1647–1652.
24. Marsh, D., Müller, M., and Schmitt, F.-J. (2000) Orientation of the infrared transition moments for an α-helix. *Biophys. J. 78*, 2499–2510.
25. Marsh, D., and Páli, T. (2001) Infrared dichroism from the X-ray structure of bacteriorhodopsin. *Biophys. J. 80*, 305–312.
26. Esmann, M., and Marsh, D. (1985) Spin-label studies on the origin of the specificity of lipid-protein interactions in Na^+,K^+-ATPase membranes from *Squalus acanthias*. *Biochemistry 24*, 3572–3578.
27. Pates, R. D., and Marsh, D. (1987) Lipid mobility and order in bovine rod outer segment disk membranes. A spin-label study of lipid-protein interactions. *Biochemistry 26*, 29–39.
28. Marsh, D., Watts, A., and Barrantes, F. J. (1981) Phospholipid chain immobilization and steroid rotational immobilization in acetylcholine receptor-rich membranes from *Torpedo marmorata*. *Biochim. Biophys. Acta 645*, 97–101.
29. Haris, P. I., and Chapman, D. (1988) Fourier transform infrared spectra of the polypeptide alamethicin and a possible structural similarity with bacteriorhodopsin. *Biochim. Biophys. Acta 943*, 375–380.
30. Haris, P. I., Molle, G., and Duclohier, H. (2004) Conformational changes in alamethicin associated with substitution of its α-methylalanines with leucines: A FTIR spectroscopic analysis and correlation with channel kinetics. *Biophys. J. 86*, 248–253.
31. Stella, L., Burattini, M., Mazzuca, C., Palleschi, A., Venanzi, M., Coin, I., Peggion, C., Toniolo, C., and Pispisa, B. (2007) Alamethicin interaction with lipid membranes: A spectroscopic study on synthetic analogues. *Chem. Biodiversity 4*, 1299–1312.
32. Horváth, L. I., Heimburg, T., Kovachev, P., Findlay, J. B. C., Hideg, K., and Marsh, D. (1995) Integration of a K^+ channel-associated peptide in a lipid bilayer: Conformation, lipid-protein interactions, and rotational diffusion. *Biochemistry 34*, 3893–3898.
33. Anbazhagan, V., Qu, J., Kleinschmidt, J. H., and Marsh, D. (2008) Incorporation of outer membrane protein OmpG in lipid membranes. Protein-lipid interactions and β-barrel orientation. *Biochemistry 47*, 6189–6198.
34. Anbazhagan, V., Vijay, N., Kleinschmidt, J. H., and Marsh, D. (2008) Protein-lipid interactions with *Fusobacterium nucleatum* major membrane protein FomA: Spin-label EPR and polarised infrared spectroscopy. *Biochemistry 47*, 8414–8423.
35. Ramakrishnan, M., Jensen, P. H., and Marsh, D. (2006) Association of α-synuclein and mutants with lipid membranes: Spin-label ESR and polarized IR. *Biochemistry 45*, 3386–3395.
36. Miick, S. M., Martinez, G. V., Fiori, W. R., Todd, A. P., and Millhauser, G. L. (1992) Short alanine-based peptides may form 3_{10}-helices and not α-helices in aqueous solution. *Nature 359*, 653–655.

37. Martinez, G., and Millhauser, G. (1995) FTIR spectroscopy of alanine-based peptides: Assignment of the amide I′ modes for random coil and helix. *J. Struct. Biol. 114*, 23–27.
38. Jackson, M., Haris, P. I., and Chapman, D. (1989) Conformational transitions in poly(L-lysine): Studies using Fourier transform infrared spectroscopy. *Biochim. Biophys. Acta 998*, 75–79.
39. Fox, R. O., Jr., and Richards, F. M. (1982) A voltage-gated ion channel model inferred from the crystal structure of alamethicin at 1.5 Å resolution. *Nature 300*, 325–330.
40. Crisma, M., Peggion, C., Baldini, C., MacLean, E. J., Vedovato, N., Rispoli, G., and Toniolo, C. (2007) Crystal structure of a spin-labelled, channel-forming, alamethicin analogue. *Angew. Chem., Int. Ed. 46*, 2047–2050.
41. Barth, A. (2000) The infrared absorption of amino acid side chains. *Prog. Biophys. Mol. Biol. 74*, 141–173.
42. Chirgadze, Y. N., Fedorov, O. V., and Trushina, N. P. (1975) Estimation of amino acid residue side-chain absorption in the infrared spectra of protein solutions in heavy water. *Biopolymers 14*, 679–694.
43. Karle, I. L., and Balaram, P. (1990) Structural characteristics of α-helical peptide molecules containing Aib residues. *Biochemistry 29*, 6747–6756.
44. Gessmann, R., Brückner, H., and Petratos, K. (2003) Three complete turns of a 3_{10}-helix at atomic resolution: The crystal structure of Z-$(Aib)_{11}$-OtBu. *J. Pept. Sci. 9*, 753–762.
45. Bak, M., Bywater, R. P., Howy, M., Thomsen, J. K., Adelhorst, K., Jakobsen, H. J., Sørensen, O. W., and Nielsen, N. C. (2001) Conformation of alamethicin in oriented phospholipid bilayers determined by ^{15}N solid-state nuclear magnetic resonance. *Biophys. J. 81*, 1684–1698.
46. van der Wel, P. C. A., Strandberg, E., Killian, J. A., and Koeppe, R. E., II (2002) Geometry and intrinsic tilt of a tryptophan-anchored transmembrane α-helix determined by ^{2}H NMR. *Biophys. J. 83*, 1479–1488.
47. Marsh, D. (2006) Elastic curvature constants of lipid monolayers and bilayers. *Chem. Phys. Lipids 144*, 146–159.
48. Ramakrishnan, M., Qu, J., Pocanschi, C. L., Kleinschmidt, J. H., and Marsh, D. (2005) Orientation of β-barrel proteins OmpA and FhuA in lipid membranes. Chainlength dependence from infrared dichroism. *Biochemistry 44*, 3515–3523.
49. Peelen, S. J. C. J., Sanders, J. C., Hemminga, M. A., and Marsh, D. (1992) Stoichiometry, selectivity, and exchange dynamics of lipid-protein interaction with bacteriophage M13 coat protein studied by spin label electron spin resonance. Effects of protein secondary structure. *Biochemistry 31*, 2670–2677.
50. Arora, A., Williamson, I. M., Lee, A. G., and Marsh, D. (2003) Lipid-protein interactions with cardiac phospholamban studied by spin-label electron spin resonance. *Biochemistry 42*, 5151–5158.
51. Cornea, R. L., Jones, L. R., Autry, J. M., and Thomas, D. D. (1997) Mutation and phosphorylation change the oligomeric structure of phospholamban in lipid bilayers. *Biochemistry 36*, 2960–2967.
52. Veiga, M. P., Arrondo, J. L. R., Goñi, F. M., Alonso, A., and Marsh, D. (2001) Interaction of cholesterol with sphingomyelin in mixed membranes containing phosphatidylcholine, studied by spin-label ESR and IR spectroscopies. A possible stabilization of gel-phase sphingolipid domains by cholesterol. *Biochemistry 40*, 2614–2622.
53. Collado, M. I., Goñi, F. M., Alonso, A., and Marsh, D. (2005) Domain formation in sphingomyelin/cholesterol mixed membranes studied by spin-label electron spin resonance spectroscopy. *Biochemistry 44*, 4911–4918.
54. Gordon, L. G. M., and Haydon, D. A. (1972) The unit conductance channel of alamethicin. *Biochim. Biophys. Acta 255*, 1014–1018.
55. Boheim, G., Hanke, W., and Eibl, H. (1980) Lipid phase transition in planar bilayer membrane and its effect on carrier- and pore-mediated ion transport. *Proc. Natl. Acad. Sci. U.S.A. 77*, 3403–3407.
56. Marsh, D. (2007) Lateral pressure profile, spontaneous curvature frustration, and the incorporation and conformation of proteins in membranes. *Biophys. J. 93*, 3884–3899.
57. Marsh, D. (2008) Protein modulation of lipids, and *vice-versa*, in membranes. *Biochim. Biophys. Acta 1778*, 1545–1575.

BI801279N